

Distributed active demand response system for peak power reduction through load shifting

G. BENYSEK¹, M. JARNUT¹, SZ. WERMINSKI^{1*}, and J. BOJARSKI²

¹Faculty of Electrical Engineering, Computer Science and Telecommunications,
University of Zielona Góra, 9 Licealna St., 65-417 Zielona Góra

²Faculty of Mathematics, Computer Science and Econometrics, University of Zielona Góra, 9 Licealna St., 65-417 Zielona Góra, Poland

Abstract. The large variability in power consumption in electrical power systems (EPS) influences not only growth balance losses and technical losses, but also in some cases reduces energy security. Delayed restoration of power generation, combined with unpredictable weather events leading to the loss of generating power can lead to a situation in which to save the stability of the power system there must be introduced in the system a load power limit or even disconnection of end-user in a given area, which will significantly reduce the comfort of use of energy. This situation can be prevented through either the building of new intervention power units or the aggregated use of new energy technologies, such as distributed network resources (DER), which are part of an intelligent Smart Grid network. Such resources bring together virtual power plants (VPP) and demand side management (DSM). The article presents an alternative decentralized active demand response (DADR) system, that by acting on selected groups of loads reduces peak loads with minimized loss of comfort of energy in use for the end-user. The system operates without any communication. The effectiveness of the proposed solution has been confirmed, outlined in test results obtained by the authors from a developed analytical model, which also contains stochastic algorithms to decrease the negative impact of such DSM systems on the power system (power overshoot and oscillation).

Key words: power system, demand-side management, load shifting, thermostatic devices.

1. Introduction

Due to the increasing standard of living and rapid technological advances there is a greatly increased demand for electricity. The nature of electricity users depends on the time of year, the type of day (working or weekend) and *ad hoc* responses to the current weather. Consequently, the power demand curve in the EPS forms valleys and peaks. These problems are the cause of financial losses in the EPS, therefore the aim is to equalize the power curve [1]. Processes used to regulate the demand-side electricity are called demand side management (DSM)/demand side response (DSR) and have been an issue described in the literature for years [2–7].

In the Polish EPS, where the so-called baseline supply uses coal-fired power plants, equalization of the daily load curve leads indirectly to increased energy efficiency in the generation sector. The greatest relative difference between peak load and the minimum load in the Polish EPS occurs in the winter, with a value of about 25% and is one of the highest in Europe. Taking into account coal-fired and lignite power plants, this results in the average efficiency of coal-fired power plants reaching 34% during peak hours and falling to approx. 31% during the night valleys hours. Reducing peak loads in the EPS may lead firstly to a reduction of grid losses, which in the Polish EPS amount to approx. 7% [8] and improve the stability of EPS by increasing the power reserve. This is particularly important

with respect to the ongoing modernization and renovation of power generation in the Polish EPS.

Due to the structure of energy production in the Polish EPS, where the vast majority of installed power generators (about 85% [9]) are thermal power plants, even the construction of new power plants would be not able to fully guarantee the safety of the EPS, moreover it is an expensive solution, approx. 780 EUR/MWh [10]. An example illustrating this fact would be the situation which occurred in August 2015, when as a result of unforeseen prolonged drought there were significantly decreased water resources available in Polish rivers which are commonly used in technological processes of thermal power plants (which exclude the operation of pumped-storage hydroelectricity and hindered cooling primary power generation power plants). This resulted in the need for load power limits to a large number of industrial customers for a period of about two weeks, causing considerable losses resulting from idle production lines. The targeted amount of power reduction was estimated at 1 GW, which is approx. 4% of the peak load on the Polish EPS.

Given the above, TSO launched commercial DSM service elements in the form of several reduction packages. Within each package the TSO is entitled to a maximum of 15 four-hour reductions in the period of 24 months service in the respective months of the offered package reduction. The TSO request may involve no more than one reduction during the day and not more than 3 weeks reduction. The program is aimed at bidders (aggregators or industrial) who have a power reduction exceeding 10 MW, and the execution of the service is billed on the basis

*e-mail: s.werminski@iee.uz.zgora.pl

Table 1
Characteristic reduction packages in the TSO program (PGE, PKN, ENSPIRION - Polish companies participating in tenders)

Reduction package	Required reduction power [MW]	Potential period reduction [month]	Price reached in tenders [EUR/MWh netto]
IA	10 – 20	X – III	220 (PGE)
IB	10 – 20	IV – IX	220 (PGE) – 1450 (PKN)
IIA	21 – 35	X – III	270 (ENSPIRION)
IIB	21 – 35	IV – IX	270 (ENSPIRION)
IIIA	36 – 55	X – III	250 (PGE)
IIIB	36 – 55	IV – IX	250 (PGE)
IVA	56 – 90	X – III	270 (ENSPIRION)
IVB	56 – 90	IV – IX	270 (ENSPIRION)

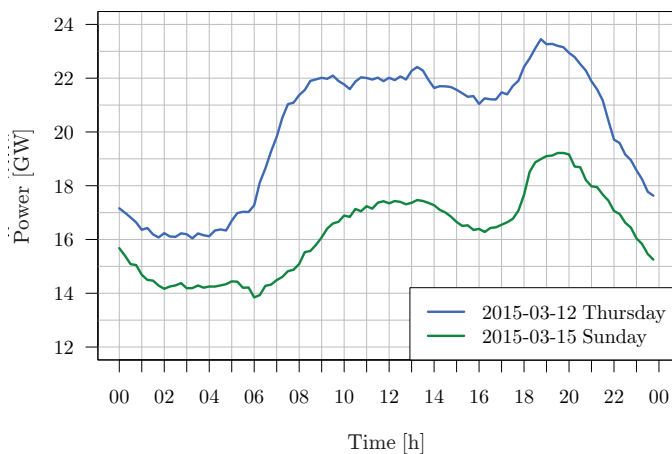


Fig. 1. Daily load curve in Polish EPS on a working and a weekend day

of the volume of energy that as a result of the service has not been downloaded from the power system. The offered price reduction for services reaches the average value of 270 EUR/MWh net (on the basis of tenders listed in Table 1). The offer is addressed mainly to the demand side Aggregators and large energy consumers. The main disadvantage of this solution is the significant cost of power reduction service intervention (approx. 270 EUR/MWh) and the limited number of reductions which may be required in the framework of the concluded contract. Moreover, any reduction is associated with the loss of energy use comfort by the end-user and can be done with a much earlier notification. Taking into account the results of the analysis of the energy consumption structure – the daily load curves in EPS (Fig. 1) and the electricity consumption profiles (Fig. 2) – it can be seen that a significant share in evening peak power is taken by small end-user (G11 tariff) and companies (C11 tariff). This leads to the conclusion that the effective reduction of peak load power in the evening peak load period can be carried out thanks to the commitment to the re-

duction of smaller energy consumers (households). Such action, because of the considerable power dissipation intervention (a large number of end-user participating in the reduction program) must be stimulated, for example, through tariffs or technically aggregated, which may create legitimate concerns as to the effectiveness of the service. The easiest action in energy consumption is reduction, but, in addition, reduction of the power demands of the small end-users (households) can be achieved by reducing the energy consumption through the use of devices with a high energy efficiency index (EEI) class [11–13] (this restriction has been introduced in the EU area) and in most cases the required class is higher than A [11]. Such action achieves a reduction of up to 60% (due to the difference in energy consumption of the EEI class D and EEI class A) especially in domestic lighting systems which contribute significantly to the generation of evening peak power.

Issues associated with controlling the Demand Side Response of small end-users are widely described in the literature [14, 15]. However, in most cases they relate the impact on the

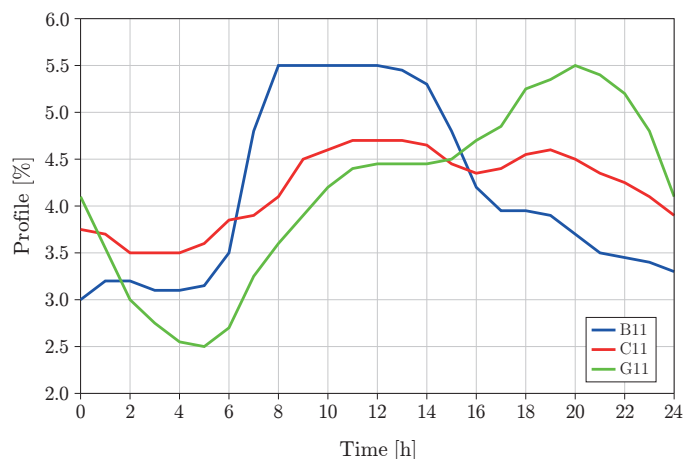


Fig. 2. Electricity consumption profile – single-zone tariff (B11, C11, G11)

demand side through tariff programs such as time of use (ToU), real time pricing (RTP) or critical peak pricing (CPP), where the price of electricity varies during the day and is associated with energy prices on the balancing market. With these tariffs the user, under pressure from high energy bills at peak times, is forced to modify his energy profile, which does not always achieve the desired effect of reducing peak loads, but may cause an increase in charges for energy bills and as a consequence the abandonment of such a program tariff [4, 16]. The concomitant changes in prices on the balancing market can also be achieved by using hardware solutions that automate demand control processes:

- centralized systems using additional information communication technology (ICT) infrastructure, such as advanced metering infrastructure (AMI) and home area network (HAN), where on the basis of current or ad-hoc information on changes in the energy price the controller performs scheduling operations for individual devices on the basis of established algorithms and priorities. This control is often called the direct load control (DLC [17, 18]);
- distributed systems using smart appliance loads with programmable operating characteristics, where the daily work schedule of equipment is determined by the internal controller or additional external device – Active Socket placed between the grid side and the controlled device [19].

The first of the described solutions, for the effective implementation of power reduction, stimulated by tariff signals, requires the use of an ICT infrastructure consisting of at least one central controller, several controlled plug-ins (two or three of the most energy-intensive loads) and a modem for communication with the AMI meter or provision of external communication through an alternative channel. The cost of such a system, based on market data is estimated by the authors to about 700 EUR.

For example, in “Real-time price-based home energy management scheduler” [20] the authors discuss home energy management, which reduces energy use by means of a price signal. In the above mentioned solutions, loads are managed by a controller which uses a stochastic algorithm to select loads at a given home to be switched on/off. The disadvantage of this solution is the lack of studies on the aggregate impact of such action, which may lead to power overshoot and oscillations. Similar analyses mainly focused on dwellings are also considered in [21–24].

In this regard, the proposed DADR system, which is dedicated to small end-users, becomes effectively a response for the demand reported by the TSO (achieving peak power reduction by 1 GW) and is responsible for the stability of the Polish EPS, moreover it may constitute an alternative or supplement to the reduction intervention program targeted at demand-side aggregators. The distinguishing feature of the DADR system is the lack of a master communication infrastructure and lack of communication between devices. The control algorithm uses probabilistic methods, which in effect eliminate power overshoot and oscillations in the EPS during synchronous switching ON and OFF of devices at the same time. The proposed solution reduces the level of power during peak hours, however, its dis-

advantage is the lack of possibility for power reduction at the TSO’s request (e.g., emergency state). Nevertheless, the lack of communication and the need for dedicated loads makes this solution relatively quick to implement and allows for the provision of services within the DSM in accordance with TSO expectations.

The system proposed in the paper is presented in the context of the Polish EPS, but may be applicable to other systems. The main contribution is to show its potential and specificity of action which stands out by its lack of communication system while at the same time not causing power overshoot and oscillation.

2. The concept of the decentralized DADR system

A characteristic feature of the DADR system shown in Fig. 3(a) is the considerable dispersion throughout the EPS and the lack of communication between its elements (DADR devices). A DADR device (Fig. (b)) has the functional ability to improve both the dynamic system stability (load frequency control – LFC block) and peak power reduction (DSR block).

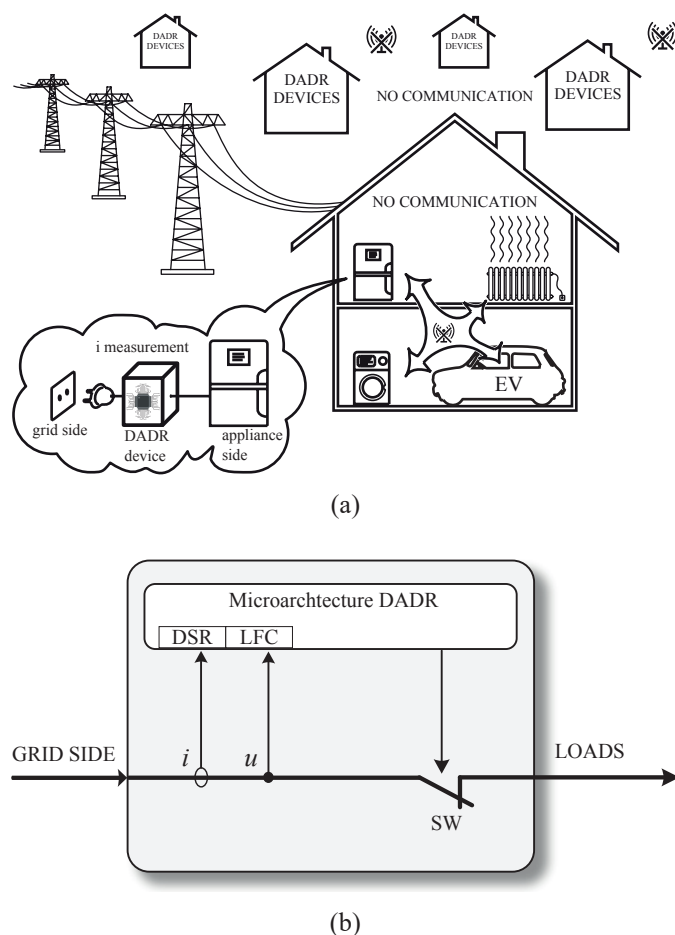


Fig. 3. DADR system as part of a DSM dispersion system: (a) DADR system concept, (b) simplified internal structure of a DADR device

In the first case the voltage frequency is measured and, based on this measurement, a working stochastic algorithm is established. In the DSM case a working algorithm based on the current measurement of the load is established -the algorithm determines the operating status of the load and time since the last ON state.

A single DADR device acting as an active intermediate socket, in which the controlled device (fridge-freezers) current, and the device’s period of work is measured, allows for the provision of services within the DSM thanks to it being equipped with a stochastic algorithm (program) which triggers the blocking operation of the powered device at certain hours of the day (peak hours). At the same time the schedule and duration of locks is correlated with the daily load curve. Moreover, the algorithm should also take into account the devices specificity of operation as well as weekly and annual variability of EPS load profile. The DADR system zone can be linked with fluctuations in load by:

- fixed schedule peak hours entered into the device memory, based on data analysis of the preceding year;
- peak hours detection based on ongoing analysis of the voltage of the EPS (RMS and/or frequency).

The first method is simpler and, as research shows, a significant dependency between the location of EPS peak load zones and the solar activity gives fairly good results, which are used among other things in determining the price zones in the impact programs on the demand side (multi-zone tariffs). The second option requires an assessment of the two-way correlation between system load and grid voltage parameters (RMS/frequency). In further analysis to determine the peak

load zone of the EPS the method used employed an array of zones permanently entered into the DADR device memory.

3. Classification of loads

3.1. Operating characteristics of loads. DSR systems perform their functions by reducing load power. In end user electric installations one rarely meets loads with regulated power, hence power limitation processes are implemented mostly by turning off selected devices or by temporary blocking of their work (time shift). Loads occurring in end user installations on the basis of their operating characteristics can be divided into three basic types [25]:

1. Baseline loads (e.g., lighting, computing, network devices);
2. Burst load (e.g., clothes dryer, dishwasher, washing machine);
3. Regular load (thermostatic devices, such as refrigerator, water heater etc.).

Baseline loads from the first group serve basic living needs (e.g., lighting) so these loads are not particularly suitable for performing functions related to the equalization of the daily load curve, but they can be part of pro-efficiency action by promoting devices with a high EEI class and by blocking “Stand-by” mode. For the purposes of demand management the two other groups are suitable devices. They differ in their nominal power, their daily work characteristics and dissemination in households [26]. A summary of parameter characteristics of devices together with an assessment of their predisposition in DSR processes is shown in Table 2.

Table 2
Types of devices in terms of of participation in DSM program

Loads		Dissemination [%] [26]	Average unit power [kW] [26]	Operating Characteristics	Mode of participation in DSM program	The theoretical value of the power reduction [GW]
Regular	Refrigerator, refrigeratorfreezer, freezer	99.50	0.08	Type 3	blockade	1.11
	HVAC	0.35	2.0 – 6.0	Type 3	blockade	0.20
	Electric water heaters or electrical therms	23.00	1.5 – 3.5	Type 3	blockade	8.05
	Electric furnaces	5.40	4.0 – 48.0	Type 3	blockade (1) / time shift (2)	19.66
	Heat pump	0.05	3.5 – 16.0	Type 3	blockade	0.07
Burst	Washing mashine	88.90	2.0 – 2.5	Type 2	time shift	28.00
	Dryer	2.00	1.0 – 3.0	Type 2	time shift	0.56
	Dishwashers	20.00	2.0 – 2.5	Type 2	time shift	6.30
1-refers convection ovens; 2-refers storage heater						

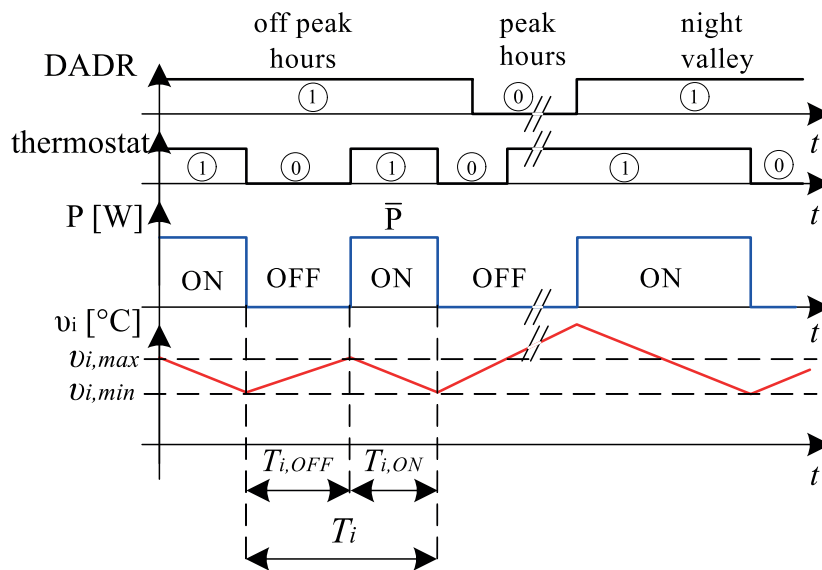


Fig. 4. The general concept of DADR action. An idealized time characteristic in normal mode and during the operational time period of DADR device.

The literature on activities describing the modification of the daily load curve of the EPS presents three basic types of control for devices, with time versus power characteristics:

- timed reduction of instantaneous power;
- shortened work cycle (average power cycle);
- intentional time shift in operational cycle of devices.

It should be noted that not all types of controls listed above for the reduction of load power equate to a reduction of final energy consumption. Possible types of controls for specific groups of devices are summarized in Table 2 (the column “The theoretical value of the power reduction” shows calculations for power values resulting from load power (mid-range value) and dissemination. In practice, these values will be lower because of the lack of simultaneity of use (to a value of approximately 50%).

3.2. Selection of loads for control via the DADR system in DSM mode. A three-level scale of predisposition to DSM presented in Table 2 takes into account criteria such as:

- the accumulated value of the power reduction, which is a derivative of the distribution of the group in the EPS and a device’s average unit power as one of the group;
- the duration and energy of a device’s single cycle operation;
- the availability for DSM action (during the day as well as during the year);
- the ability to exert influence on the characteristics of a device’s operation without interfering with its construction;
- the subjective volume of discomfort felt by the user, caused by the participation of the particular type of device involved in DSM actions.

As can be seen from the results of the evaluation listed in the last column of Table 2, sometimes, despite possessing high

technical predispositions, a low rating for a given group of devices (e.g., heat pumps and HVAC systems) is determined by low dissemination in the Polish EPS. On the other hand low unit power with high availability and a low rate of loss of comfort makes devices such as refrigerators (fridge-freezers or freezers) a target group of devices for control by the DADR system. Considering the above, further studies will be focused on freezers. The main reason for the use of such devices is their ubiquity and daily availability from the point of view of the provision of DSM services. According to data from the Polish Central Statistical Office [26] refrigerators and freezers are used in 99.5% of Polish households (Table 2).

3.3. Switching off thermostatically controlled devices to serve reduction of peak power load. Controlling thermostatic devices, in order to improving the performance of the EPS is widely described in the literature [27–34]. However, these solutions often require interference in the structure of the devices (e.g., a forced change of temperature range delimits in the aggregate), which action is possible through communications (Smart Grid) [1, 15 35–42]. The advantage of the proposed DADR system is that there is no interference in the structure of the device and no communication between the elements of the system (DADR devices).

Taking into account the above, freezers have been selected for further analysis. The use of these devices in the provision of DSM services requires the blocking of the operation of their aggregates at peak hours (Fig. 4). During off-peak hours the DADR system allows the freezer to operate in its normal mode. In most cases, due to the inertia of these processes, disabling them for a period not exceeding 2 – 3 hours (about 2 – 3 operating cycles) does not cause a significant loss of their functionality, but larger control temperature deviations have to be reckoned with.

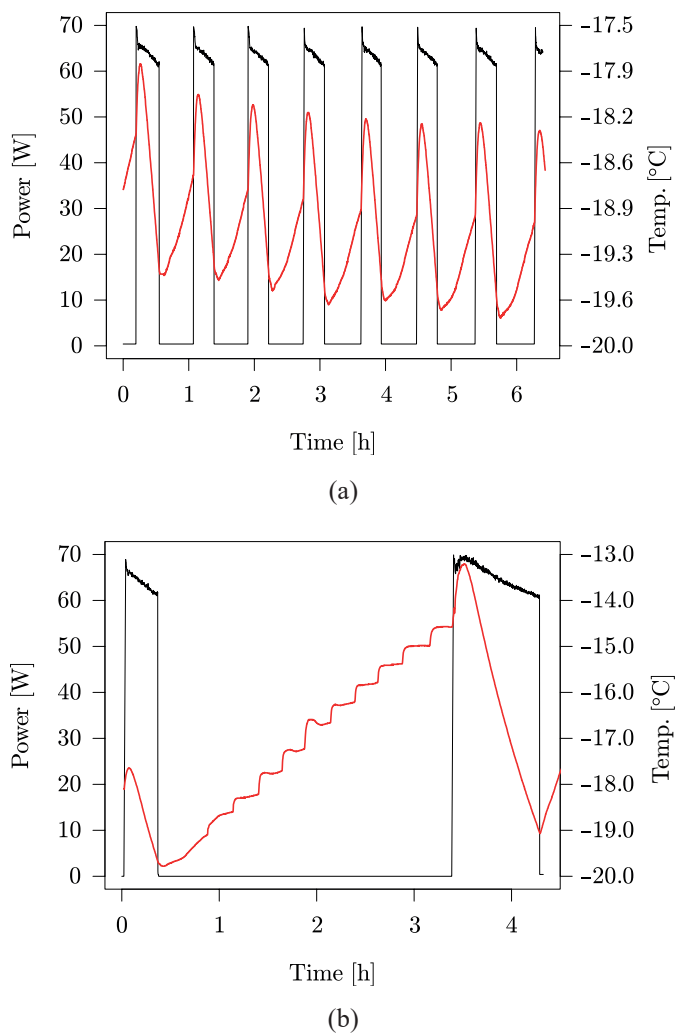


Fig. 5. Characteristics of power consumption and freezer temperature over time: (a) normal mode, (b) three hour power off mode (with door opening at 15 minute intervals for 20 sec.)

As shown in the measurements in normal mode the operating temperature on a freezer’s middle shelf varies from -19.8°C to -17.5°C (Fig. 5(a)). In a situation in which the freezer is turned off for 3 hours (2 – 3 operation cycles) and where the door is not opened, the temperature rises to -16.3°C . Opening the door every 15 minutes for 20 seconds (which is above typically frequency of openings) causes the temperature in the freezer to rise to -13.3°C (Fig. 5(b)). However, regardless of the manner of usage (even when a device is turned off for several hours), there is no degradation of the operation that would threaten to render the products unusable.

4. Stochastic control algorithm

4.1. Normal freezer operation cycle. Assume that each i -th is a typical controlled device operation cycle by a DADR device and consists of two consecutive steps. The first step OFF (aggregate off) starts after reaching minimum temperature v_{\min} .

Then the aggregate is switched off for a period of $T_{i, \text{OFF}}$. After reaching the maximum temperature ϑ_{\max} , the device cycle proceeds to the second stage of ON (aggregate on). The device operates for a period $T_{i, \text{ON}}$, with average power \bar{P} , to achieve a minimum temperature ϑ_{\min} . Assume that the operating time period of the aggregate $T_{i, \text{ON}}$ to reduce the temperature inside the freezer to the level of ϑ_{\min} is proportional to the aggregate switch-off time [30, 32, 33], which can be written as

$$T_{i, \text{ON}} = \alpha T_{i, \text{OFF}}, \quad (1)$$

where $\alpha > 0$ is the coefficient of proportionality.

Moreover due to the asynchronous operation of individual devices it is assumed that the period in which the aggregate of the i -th device does not work is aleatory with uniform distribution in the range from T_{\min} to T_{\max} , which is denoted $T_{i, \text{OFF}} \sim \mathcal{U}(T_{\min}, T_{\max})$. This means that the operating period of the aggregate of the i -th device is also a random variable with uniform distribution $T_{i, \text{ON}} \sim \mathcal{U}(\alpha T_{\min}, \alpha T_{\max})$.

4.2. Freezer operational cycle during the operational time period of DADR device. As mentioned earlier the main task of the DADR device is the interruption of freezer operational states for a specified period of time during peak load instances. Accordingly, the DADR devices must have a cache in which is stored the peak hour schedules for the whole year, as well as a real time clock, a stopwatch (which measures time elapsed from changes in operating status) and a pseudo-random number generator module. Using stochastic techniques for the control algorithm (Fig. 6) this will prevent the synchronous switch-on

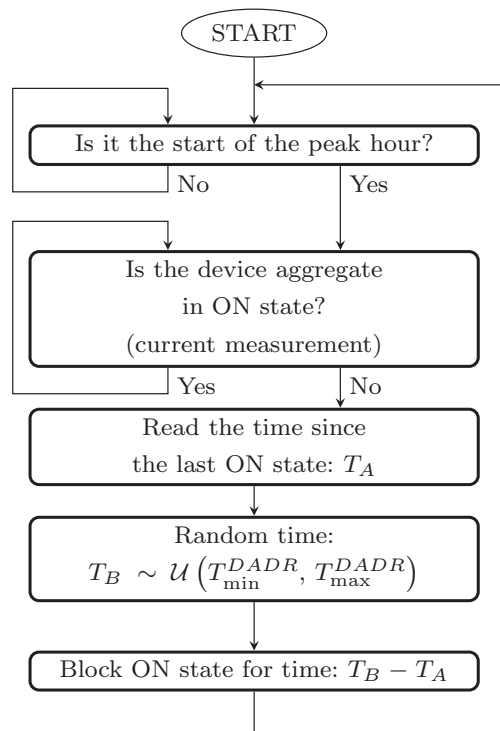


Fig. 6. The DADR device operational algorithm in DSM mode

of blocked devices after the peak period, which would result in power oscillations in the EPS [30].

At the start of the algorithm (Fig. 6) the DADR device reads from the cache the peak hour start time. At the start of the peak period, the cooling device operational status is checked (based on measurement of the current):

- if device aggregator is OFF, block ON state for a time difference T_B with random period based on uniform distribution and time T_A since last ON state;
- if device aggregator is ON, wait until OFF state occurs and block ON state for time T_B with random period based on uniform distribution (in this case the value of T_A is close to 0).

Considering the above in the analysis it was assumed, that the time of the forced break in the freezer aggregate operation will be random with uniform distribution $\mathcal{U}(T_{\min}^{\text{DADR}}, T_{\max}^{\text{DADR}})$, which means that the unit will be turned off for at least the period T_{\min}^{DADR} but not longer than T_{\max}^{DADR} . These periods are determined by the duration of the peak hour loading of the day.

4.3. Analysis of the stochastic algorithm operation. At any moment t randomly selected device (freezer) can be in one of two states

$$S(t) = \begin{cases} 0, & \text{when the aggregate is not working,} \\ 1, & \text{when the aggregate is working.} \end{cases} \quad (2)$$

State function $S(t)$ is a two-point random variable, whose distribution is generally unknown. However, for the assumptions described in subsection 4.1, as demonstrated in [27], the probability state function at any t moment asymptotically converges to

$$\Pr(S(t) = 0) = \frac{1}{1 + \alpha}, \quad \Pr(S(t) = 1) = \frac{\alpha}{1 + \alpha}, \quad (3)$$

which means that a randomly selected device (freezer) whose electrical profile has been modified, at randomly indicated time, operates with probability $\alpha/(1 + \alpha)$ (this relationship also determines the fill factor).

In the DADR system, by extending the modified aggregate on-state, the state function is designated as $S_{\text{DADR}}(t)$. We assume that at the time t_0 there occurs a peak load and the DADR device executes the algorithm described in Fig. 6. On the basis of assertions of total probability we can then determine the probability of the aggregate's operational mode:

$$\begin{aligned} \Pr(S_{\text{DADR}}(t) = 1) &= \\ &= \Pr(S(t) = 1 | S(t_0) = 0) \Pr(S(t_0) = 0) \\ &+ \Pr(S(t) = 1 | S(t_0) = 1) \Pr(S(t_0) = 1). \end{aligned} \quad (4)$$

Note that the assumptions concerning time periods of freezer cycle operation are based on normal distributions. Hence the

probability $\Pr(S(t) = 1 | S(t_0) = 0)$ and $\Pr(S(t) = 1 | S(t_0) = 1)$ can be determined using the distributions of random variables, which are linear combinations and products of independent random variables with normal distribution. Using the auxiliary assertions given in Appendix A it is possible to prove the correctness of the following formula, by which can be determined the probability that any thermostatic device connected to a DADR device is in an ON state at a given moment

$$\begin{aligned} \Pr(S_{\text{DADR}}(t) = 1) &= \\ &= \left(G\left((1 + \alpha)T_{\max}^{\text{DADR}} - (t - t_0); \right. \right. \\ &\quad \left. \left. T_{\min}, T_{\max}, (1 + \alpha)\Delta T^{\text{DADR}} \right) \right. \\ &\quad \left. - G\left(T_{\max}^{\text{DADR}} - (t - t_0); T_{\min}, T_{\max}, \Delta T^{\text{DADR}} \right) \right) \frac{1}{1 + \alpha} \\ &+ \left(1 - F(t - t_0; \alpha T_{\min}, \alpha T_{\max}) \right. \\ &\quad \left. + G\left(t - t_0 - T_{\min}^{\text{DADR}}; \alpha T_{\min}, \alpha T_{\max}, \Delta T^{\text{DADR}} \right) \right) \\ &\quad \cdot \frac{\alpha}{1 + \alpha}, \end{aligned} \quad (5)$$

where: $\Delta T^{\text{DADR}} = T_{\max}^{\text{DADR}} - T_{\min}^{\text{DADR}}$, F and G are defined functions in Appendix A.

An example probability state function curve $S_{\text{DADR}}(t)$ is shown in Fig. 7. As can be seen the probability curve outside the range $t_0 \leq t \leq t_0 + (1 + \alpha)T_{\max}^{\text{DADR}}$ is on a constant level $\alpha/(1 + \alpha)$, which corresponds to the probability that freezers are operating in normal mode (Fig. 3). From the moment of the onset of peak hours ($t = 0$) the probability that the aggregate operates decreases to 0. This means that all devices covered by the DADR system, after the end of their operation cycle are switched OFF. The blocking operation of all devices covered by the DADR system remains until $T_{\min}^{\text{DADR}} - T_{\max}$. Due to all the fridges being in the OFF state for T_{\min}^{DADR} to T_{\max}^{DADR} hours,

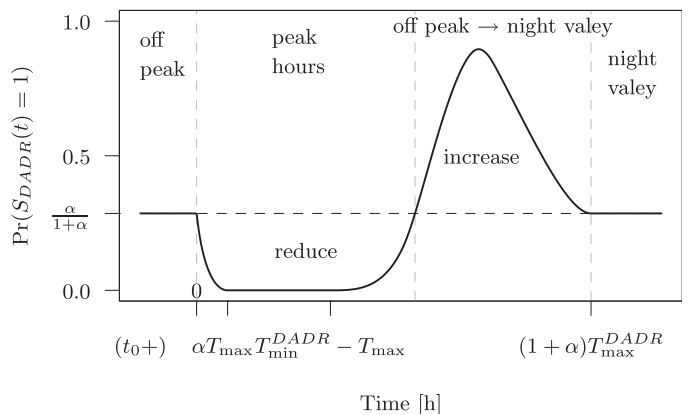


Fig. 7. The probability curve for changes in the distribution of freezers in power-on mode

their next ON state will be longer than in typical normal mode of operation (according to equation 1, Fig. 4). Moreover, all fridges will go to ON state within ΔT^{DADR} . For this reason, in the next few hours of operation of 16 mln fridges, they will be “more synchronized”, likewise the probability of the devices being in operational state rises to well above the level corresponding to the normal mode of operation. After this time (after peak hours, in the night valley – Fig. 7) operation of the 16 mln devices will naturally revert back to their natural state, before the next peak hours start.

Assuming that the DADR system covers a large number of N identical thermostatic devices and knowing the probability of a single freezer operating at any given time t , then using the property of binominal distribution we can determine the average number of operating freezers

$$\Pr(S_{DADR}(t) = 1) \cdot N, \quad (6)$$

and here we can determine the average power consumption

$$\Pr(S_{DADR}(t) = 1) \cdot N \cdot \bar{P}. \quad (7)$$

In off-peak hours, in normal mode, the probability that a freezer is operating $\alpha/(1 + \alpha)$. Hence, the maximum power that can be reduced in the DADR system is

$$P_{\text{reduce,max}} = \frac{\alpha}{1 + \alpha} \cdot N \cdot \bar{P}. \quad (8)$$

From the formula (7) we know the average of the instantaneous power devices covered by DADR system, hence reduced average energy consumption is given by

$$\begin{aligned} \bar{E}_{\text{reduce}} &= \frac{1}{2} N \bar{P} \int_0^{(1+\alpha)T_{\text{max}}^{DADR}} \left| \Pr(S_{DADR}(t) = \right. \\ &= 1) - \frac{\alpha}{1 + \alpha} \left. \right| dt. \end{aligned} \quad (9)$$

This formula allows for the calculation of energy reduction for any thermostatic device and various durations of peak hours.

5. Case study

In order to verify the properties of the proposed solution a simulation study was conducted, where we checked the aggregate impact of the DADR system intervention on the real characteristics of the daily load curve for the Polish EPS. For the simulation an assumed daily load curve from 2015–03–12 was employed. Also assumed was a 16 million population of controlled devices (the number of fridges and freezers in Polish households

according to the data from CSO [26]). An assumed average device power consumption based on measurement came to $\bar{P} = 80$ W. The minimum and maximum delay time (which is also the minimum and maximum period of operation of the aggregate in a single cycle) was also determined on the basis of the measurements, ranging from 20 to 40 minutes (these times are mostly dependent on the freezer and its manner of usage). In addition, in order to avoid simultaneous mass switching ON of devices, the time for which they were set to activate in DSM mode was randomly set according to $\mathcal{U}(T_{\text{min}}^{DADR}, T_{\text{max}}^{DADR})$ (these times are correlated with the duration of the peak hours of the day). A DSM mode activation signal was set for 18:15 for the daily load curve from 2015–03–12. Given below is a description of the parameters adopted for the simulation tests:

- population of devices involved in the service of DSM: $N = 16 \cdot 10^6$ (thermostatic number of devices based on CSO data [26]),
- average electrical power of a single device $\bar{P} = 80$ W (based on measurement and [26]),
- the moment of activation of the DSM service $t_0 = 18:15$ (based on an example at the beginning of the peak hours from 2015–03–12),
- minimum and maximum period of freezer aggregate operation $T_{\text{min}} = 20$ min, $T_{\text{max}} = 40$ min (based on measurements of the tested freezer)
- factor $\alpha = 0.35$ (characteristics of thermostatic devices [27–34])
- minimum and maximum activation period of devices in DSM mode: $T_{\text{min}}^{DADR} = 120$ min, $T_{\text{max}}^{DADR} = 180$ min (adopted on the basis of analyses carried out at point 3.3)

5.1. Results of the simulation and evaluation of energy performance. Considering the above data and the formula determined in subparagraph 4.3 the impact of the DADR system on the daily load curve the Polish EPS was calculated, taking into account the proposed stochastic algorithm (Fig. 8(a)) as well as the deterministic approach encountered in the literature [27–34] (Fig. 8(b)).

In Fig. 8(b) and 8(a) t_1 is the beginning of power reduction. As can be observed in the deterministic algorithm there is power overshoot. At the end of power reduction, in point t_2 , demand for energy switch OFF of aggregated devices is greater, but in the deterministic approach we have power overshoot again, and after that, oscillation due to the simultaneity of operating 16 mln fridges (over time simultaneity is “blurred” and oscillations decrease).

The simulation results show that the use of the DADR system in a population of 16 million participating devices in the DSM program reduces peak power by 0.37 GW (1.6% from targeted 4%) and reduces energy consumption at peak hours by about 0.65 GWh. Simultaneously, it should be noted that in thermostatically controlled devices, in accordance with considerations referred to in point 3.3, after deactivating the DADR system this energy is progressively “received” from the EPS causing a temporary loading of the EPS and filling in of parts of the off-peak zone. Due to the short time zones of DSM and the increased power consumption immediately after the DSM zone (about 3 hours) both power reduction and increased power

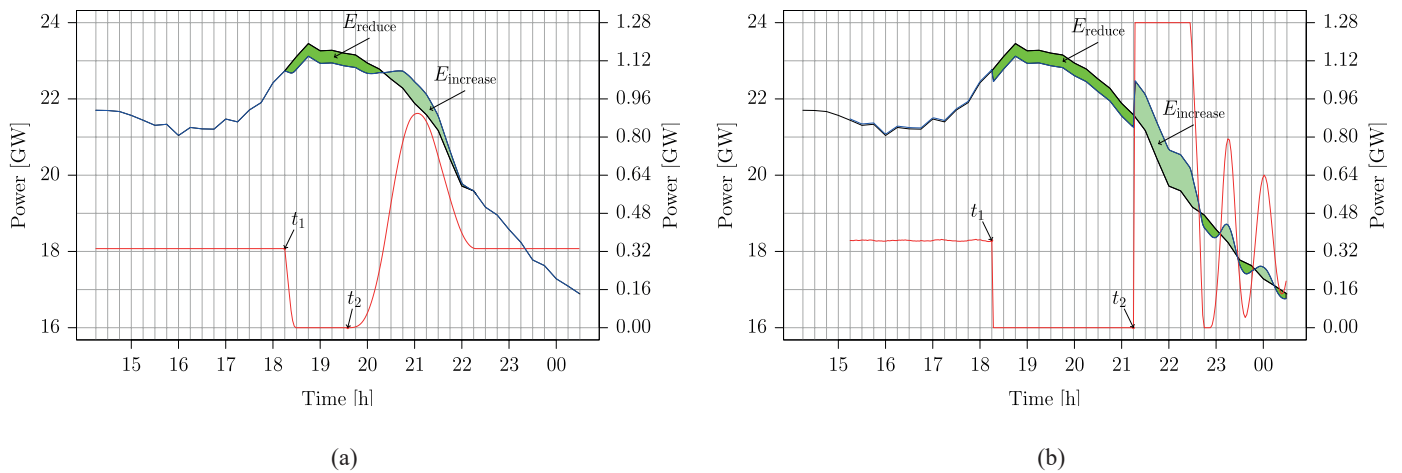


Fig. 8. The simulation results of the DADR system in DSM mode: (a) with stochastic algorithm, (b) without stochastic algorithm, where: DADR – the reduction potential of devices covered by the DADR system; EPS – daily load curve of Electrical Power System in Poland; EPS + DADR – the daily load curve of EPS taking into account the DADR system activity; E_{reduce} , $E_{increase}$ – areas corresponding respectively to reduction and greater consumption of electricity upon activation of the DADR system

demand occur in the EPS load zone at a level above the average power demand. This means that the DADR system may lead to a reduction of the transmission power loss by reducing peak power and peak current values.

Table 3 shows reduced values of energy for different cycle times of thermostatic devices, various coefficients for α and various durations of peak hours, calculated from the equation (9). The first case ($\alpha = 0.35$) is from the illustrated simulation (Fig. 8(a)), but equation (9) allows for the calculation of the reduced amount of energy for different parameters. It can be seen that devices covered by the DADR system which have a longer operating time in comparison to standby time (greater factor α) can produce an increase in the amount of possible energy reduction. Similarly, in the case of increasing the random period for switching off devices – T_{min}^{DADR} and T_{min}^{DADR} – there is an increase in the amount of energy reduction.

6. Summary

The article has presented the basic assumptions on the use of the DADR system to reduce peak loads. The advantage of the proposed solution is its lack of communication between system components and lack of need to interfere in the internal structure of controlled devices. The outcomes of the study show the relationships which allow for the calculation of the amount of reduced energy for different devices characterized by cyclical operation, for various operating characteristics of these devices and various peak hour durations. The simulation research on the developed control algorithm has demonstrated the ability to eliminate the adverse impacts (power overshoot and oscillations) on the EPS, as is the case with traditional DSM systems based on unconditional power reduction. Simultaneously it can be seen that by using a selected, sufficiently large pop-

Table 3

The reduction in consumption of electrical energy, dependent on the parameter characteristics of thermostatic devices and various time durations of peak loads

l.p.	T_{min} [min]	T_{max} [min]	α	T_{min}^{DADR} [min]	T_{max}^{DADR} [min]	\bar{E}_{reduce} [GWh]
1	20.00	40.00	0.35	120.00	180.00	0.65
2	25.00	40.00	0.40	120.00	180.00	0.65
3	25.00	40.00	0.60	120.00	180.00	0.88
4	25.00	40.00	0.40	150.00	210.00	0.84
5	20.00	30.00	0.40	120.00	180.00	0.69
6	20.00	30.00	0.60	120.00	180.00	0.93

Table 4
Actions for peak power reduction

Type of action	The construction of new generating power plants	Reduction programs (tariffs)	HAN	DADR
Cost of balance service	780 EUR/MWh	340 EUR/MWh	difficult to determine	270 EUR/MWh
Demand side response effectiveness	high	high (DLC) / low (tariff programs)	high	high
Comfort reduction	none	high	low / high (depends on defined scenario)	low
Ability to “soft start” and “soft stop” action	possible	possible	possible	possible

ulation of relatively low powered devices it is possible to bring about the desired result of power reduction – approx. 0.37 GW – without significantly impairing their functionality. With such an operation TSO expectations can be met, with an intermediate target of 0.2 GW reduction in power during peak hours, and a final goal of 1 GW. As a result of power reduction during peak hours, energy is shifted (reduced from peak hours and increased in the night valley – see Table 3, Fig. 8). As can be seen from Table 3 the value of reduced energy varies from 0.65 GWh to 0.93 GWh and this depends on the nature of the operation of loads (refrigerators) and duration of peak hours. This meets TSO expectations, which is, for example, a reduction of about 0.4 GWh (intermediate targets) over two-hours at peak hour periods. Simulations show the high potential of such action.

Properties of particular reduction techniques summarized in Table 4 show that the DADR system, because of its very simple construction, is also characterized by the lowest cost of reduction service among solutions requiring the involvement of technical measures. It also provides high reliability in reduction performance and it is relatively quick to implement.

Acknowledgements. This work has been financed from scientific research resources, referenced under project GEKON no. 213880.

A. Propositions

The appendix presents propositions from which relationship (5) is derived. Proofs are omitted because they can be carried out using the elementary theory of probability [43].

Propositions 1. Let $X \sim \mathcal{U}(A, B)$ and $Y \sim \mathcal{U}(0, 1)$ they are independent random variables. Then the cumulative distribution function (CDF) of random variables $Z = XY$ and $Z = X(1 - Y)$ has the form:

$$F(z;A,B) = \ln\left(\frac{B}{A}\right) \frac{z}{B-A} \langle_{(0,A)}(z) + \frac{(1 + \ln(\frac{B}{z}))z - A}{B-A} \langle_{(A,B)}(z) + \langle_{(B,+\infty)}(z). \tag{10}$$

Propositions 2. Let X be a random variable with CDF $F(x; A, B)$ and $Y \sim \mathcal{U}(0, C)$. In addition, it is assumed that X and Y are independent.

Then the random variable $Z = X + Y$ has the CDF:

$$G(z;A,B,C) = \frac{\ln(\frac{B}{A})}{(B-A)C} \left(\frac{1}{2} (z^2 \langle_{(0,A+C)}(z) - (z-C)^2 \langle_{(C,A+C)}(z) - (z-A)^2 \langle_{(A,A+C)}(z) + AC \langle_{(A+C,+\infty)}(z) \right) + \frac{1}{C} \left((zH_1(z) - H_2(z) - zH_1(A) + H_2(A)) \langle_{(A,B+C)}(z) - (zH_1(z) - H_2(z) - zH_1(B) + H_2(B)) \langle_{(B,B+C)}(z) - ((z-C)H_1(z-C) - H_2(z-C) - (z-C)H_1(A) + H_2(A)) \langle_{(A+C,B+C)}(z) + (CH_1(B) - CH_1(A)) \langle_{(B+C,+\infty)}(z) \right), \tag{11}$$

where

$$H_1(z) = \frac{1 + \ln(\frac{B}{z})}{B-A} z, \quad H_2(z) = \frac{1 + 2 \ln(\frac{B}{z})}{4(B-A)} z^2.$$

The next proposition is a generalization of the proposition 2.

Propositions 3. Let X be a random variable with distribution function $F(x; A, B)$ and $Y \sim \mathcal{U}(D, E)$. In addition, it is assumed that X i Y are independent. Then the random variables have the form:

1. $Z = X + Y$ with the CDF

$$G(z - D; A, B, E - D), \quad (12)$$

2. $Z = Y - X$ with the CDF

$$1 - G(E - z; A, B, E - D). \quad (13)$$

REFERENCES

- [1] M. Aunedi, P. Kountouriotis, J. Calderon, D. Angeli, and G. Strbac, "Economic and environmental benefits of dynamic demand in providing frequency regulation", *IEEE Trans. Smart Grid* 4 (4), 2036–2048 (2013).
- [2] S. N. Singh and J. Østergaard, "Use of demand response in electricity markets: An overview and key issues", in *Energy Market (EEM), 2010 7th International Conference on the European*, 1– 6 (2010).
- [3] U. D. of Energy, "Benefits of demand response in electricity markets and recommendations for achieving them", tech. rep., 2006.
- [4] "Demand side response in the domestic sector – a literature review of major trials", tech. rep., Department of Energy & Climate Change, 2012.
- [5] M. E. El-Hawary, "The smart grid–state-of-the-art and future trends, special issue: The smart grid–state-of-the-art and future trends", *Electr. Power Compo. Sys.* 4, (2014).
- [6] B. Favre and B. Peupartier, "Application of dynamic programming to study load shifting in buildings", *Energy Build.* 82 (0), 57 – 64 (2014).
- [7] T. Rajeev and S. Ashok, "Dynamic load-shifting program based on a cloud computing framework to support the integration of renewable energy sources", *Appl. Energy* 146 (0), 141 – 149 (2015).
- [8] A. Kot, W. Szypra, and J. Kulczycki, "Possibilities of losses reduction in medium voltage distribution networks by optimal network configuration", *Acta Energetica* (2), 43–59 (2009).
- [9] PSE, "Annual report 2010", tech. rep., 2010.
- [10] PSE, "Developing a model to implement DSR mechanisms on the energy market in poland. stage ii: Development of the concept of DSR mechanisms for the domestic electricity market.", tech. rep., 2010.
- [11] O. J. of the European Union, "Directive 2009/125/ec of the european parliament and of the council of 21 october 2009 establishing a framework for the setting of ecodesign requirements for energy-related products", October 2009.
- [12] O. J. of the European Union, "Directive 2010/30/eu of the european parliament and of the council of 19 may 2010 on the indication by labelling and standard product information of the consumption of energy and other resources by energy-related products", May 2010.
- [13] O. J. of the European Union, "Commission regulation (ec) no 643/2009 of 22 july 2009 implementing directive 2005/32/ec of the european parliament and of the council with regard to ecodesign requirements for household refrigerating appliances", July 2009.
- [14] J. G. Korpikiewicz, L. Bronk, and T. Pakulski, "Capabilities deliver ancillary services provided by decentralized energy generation", *Acta Energetica* 2, 70–79 (2014).
- [15] Y. Wang, Q. Chen, C. Kang, M. Zhang, K. Wang, and Y. Zhao, "Load profiling and its application to demand response: A review", *Tsinghua Sci. Technol.* 20 (2), 117–129 (2015).
- [16] X. Chen, T. Wei, and S. Hu, "Uncertainty-aware household appliance scheduling considering dynamic electricity pricing in smart home", *IEEE Trans. Smart Grid* 4 (2), 932–941 (2013).
- [17] Y. Li, B. L. Ng, M. Trayer, and L. Liu, "Automated residential demand response: Algorithmic implications of pricing-models", *IEEE Transactions on Smart Grid* 3 (4), 1712–1721 (2012).
- [18] C. Chen, J. Wang, and S. Kishore, "A distributed direct load control approach for large-scale residential demand response", *IEEE Transactions on Power Systems* 29 (5), 2219–2228 (2014).
- [19] M. Vlot, J. Knigge, and J. Slootweg, "Economical regulation power through load shifting with smart energy appliances", *IEEE Trans. Smart Grid* 4 (3), 1705–1712 (2013).
- [20] C. Vivekananthan, Y. Mishra, and F. Li, "Real-time price based home energy management scheduler", *IEEE Transactions on Power Systems* 30 (4), 2149–2159 (2015).
- [21] C. L. Su and D. Kirschen, "Quantifying the effect of demand response on electricity markets", *IEEE Transactions on Power Systems* 24 (3), 1199–1207 (2009).
- [22] A. Safdarian, M. Fotuhi-Firuzabad, and M. Lehtonen, "Integration of price-based demand response in discos' short-term decision model", *IEEE Transactions on Smart Grid* 5 (5), 2235– 2245 (2014).
- [23] Y. Ozturk, D. Senthilkumar, S. Kumar, and G. Lee, "An intelligent home energy management system to improve demand response", *IEEE Transactions on Smart Grid* 4 (2), 694– 701 (2013).
- [24] H. T. Haider, O. H. See, and W. Elmenreich, "A review of residential demand response of smart grid", *Renewable and Sustainable Energy Reviews* 59, 166 – 178 (2016).
- [25] G. Costanzo, G. Zhu, M. Anjos, and G. Savard, "A system architecture for autonomous demand side load management in smart buildings", *IEEE Trans. Smart Grid* 3 (4), 2157– 2165 (2012).
- [26] C. S. Office, "Energy consumption in households in 2012", March 2014.
- [27] D. Angeli and P. Kountouriotis, "A stochastic approach to "dynamic-demand" refrigerator control", *IEEE Trans. Control Syst. Technol.* 20 (3), 581–592 (2012).
- [28] M. Kamgarpour, C. Ellen, S. Soudjani, S. Gerwinn, J. Mathieu, N. Mullner, A. Abate, D. Callaway, M. Franzle, and J. Lygeros, "Modeling options for demand side participation of thermostatically controlled loads", *Bulk Power System Dynamics and Control – IX Optimization, Security and Control of the Emerging Power Grid*, 1–15 (2013).
- [29] P.-A. Angeli, David; Kountouriotis, "Decentralized random control of refrigerator appliances", 12144–12149 (2011).
- [30] G. Niro, D. Salles, M. V. Alcântara, and L. C. da Silva, "Large-scale control of domestic refrigerators for demand peak reduction in distribution systems", *Electr. Power Syst. Res.* 100 (0), 34 – 42 (2013).
- [31] C. Perfumo, E. Kofman, J. H. Braslavsky, and J. K. Ward, "Load management: Model-based control of aggregate power for populations of thermostatically controlled loads", *Energy Conv. Manag.* 55 (0), 36 – 48 (2012).

- [32] M. Stadler, W. Krause, M. Sonnenschein, and U. Vogel, "The adaptive fridge—comparing different control schemes for enhancing load shifting of electricity demand", *21st Conference Informatics for Environmental Protection-Enviroinfo Warsaw*, 199–206 (2007).
- [33] M. Stadler, W. Krause, M. Sonnenschein, and U. Vogel, "Modelling and evaluation of control schemes for enhancing load shift of electricity demand for cooling devices", *Environ. Modell. Softw.* 24 (2), 285 – 295 (2009).
- [34] Y. Sun, S. Wang, F. Xiao, and D. Gao, "Peak load shifting control using different cold thermal energy storage facilities in commercial buildings: A review", *Energy Conv. Manag.* 71, 101 – 114 (2013).
- [35] J. Laghari, H. Mokhlis, M. Karimi, A. Abu Bakar, and H. Mohamad, "A new under-frequency load shedding technique based on combination of fixed and random priority of loads for smart grid applications", *IEEE Trans. Power Syst.* PP (99), 1–9 (2014).
- [36] B. Shi and J. Liu, "Decentralized control and fair load-shedding compensations to prevent cascading failures in a smart grid", *Int. J. Electric Power Energy Syst.* 67 (0), 582 – 590 (2015).
- [37] M. Vedady Moghadam, R. Ma, and R. Zhang, "Distributed frequency control in smart grids via randomized demand response", *IEEE Trans. Smart Grid* 5 (6), 2798–2809 (2014).
- [38] S. Vachirasricirikul and I. Ngamroo, "Robust lfc in a smart grid with wind power penetration by coordinated v2g control and frequency controller", *IEEE Trans. Smart Grid* 5 (1), 371–380 (2014).
- [39] H. Shayeghi, H. Shayanfar, and A. Jalili, "Load frequency control strategies: A state-of-the-art survey for the researcher", *Energy Conv. Manag.* 50 (2), 344 – 353 (2009).
- [40] K. K. W. Zhang, J. Lian, L. Marinovici, C. Moya, and J. Dagle, "Distributed smart grid asset control strategies for providing ancillary services", tech. rep., Pacific Northwest National Laboratory Richland, 2013.
- [41] G. Strbac, "Demand side management: Benefits and challenges", *Energy Policy* 36 (12), 4419 – 4426 (2008).
- [42] C. Zhao, U. Topcu, N. Li, and S. Low, "Design and stability of load-side primary frequency control in power systems", *IEEE Trans. Autom. Control* 59 (5), 1177–1189 (2014).
- [43] A. N. Shiryaev, *Probability*. Springer, New York, 1996.